Shallow-depth $CaCO_3$ dissolution: Evidence from excess calcium in the South China Sea and its export to the Pacific Ocean

Zhimian Cao[1] and Minhan Dai[1]

Received 6 October 2009; revised 11 November 2010; accepted 15 February 2011; published 2 June 2011.

[1] Variations in seawater-dissolved calcium ion (Ca^{2+}) are small but substantial, which provides information essential to establish the oceanic calcium carbonate ($CaCO_3$) dissolution flux. In this study, high-precision data of Ca^{2+} were collected in the South China Sea (SCS), the largest marginal sea of the western North Pacific, and its precursor, the West Philippine Sea (WPS), on the basis of two cruises conducted in 2007 and in 2008. An excess Ca^{2+} of 13 ± 5 μmol kg^{-1} was observed in the SCS subsurface water at 200–800 m relative to the WPS, and we suggest that such an excess is attributed to in situ $CaCO_3$ dissolution at a rate of ~0.5 mmol m^{-2} d^{-1} in the SCS shallow subsurface water. Through subsurface water outflow, this shallow-depth $CaCO_3$ dissolution may provide a Ca^{2+} export flux of $(0.8 \pm 0.3) \times 10^{12}$ mol yr^{-1} from the SCS to the WPS, establishing it as an important Ca^{2+} source from the SCS to the interior Pacific Ocean. This study indicates, for the first time, that along with the benthic processes, $CaCO_3$ dissolution in waters at shallow depth in marginal seas could also contribute to Ca^{2+} and total alkalinity accumulations in the upper layer of the open ocean, which would ultimately enhance the buffer capacity of the world ocean in the context of rising anthropogenic CO_2.

Citation: Cao, Z., and M. Dai (2011), Shallow-depth $CaCO_3$ dissolution: Evidence from excess calcium in the South China Sea and its export to the Pacific Ocean, *Global Biogeochem. Cycles*, *25*, GB2019, doi:10.1029/2009GB003690.

1. Introduction

[2] The formation and dissolution of calcium carbonate ($CaCO_3$) is an important component of the oceanic carbon cycle. Recent estimates of both $CaCO_3$ production and export at a global ocean scale were roughly at the same order, at 0.4–1.8 Gt C yr^{-1}, suggesting relatively high carbon export efficiency in the form of inorganic carbon [*Berelson et al.*, 2007]. Together with organic carbon metabolism (photosynthesis and respiration), the $CaCO_3$ cycle modulates the oceanic dissolved inorganic carbon system and eventually the CO_2 buffer capacity of the world ocean. Relevant issues have also emerged concerning the fate of $CaCO_3$ and calcifiers in the context of ocean acidification that has occurred since the last century [*Intergovernmental Panel on Climate Change*, 2007]. Several studies have indicated that biogenic calcification will decline and $CaCO_3$ dissolution will increase under rising atmospheric CO_2 and lowered seawater pH [*Kleypas et al.*, 1999; *Riebesell et al.*, 2000; *Zondervan et al.*, 2001; *Andersson et al.*, 2005; *Delille et al.*, 2005; *Orr et al.*, 2005]. As a consequence, the oceanic $CaCO_3$ export will decrease, which might further weaken its ballast effect for vertical transfer of organic carbon to the deep ocean [*Armstrong et al.*, 2002; *Barker et al.*, 2003].

[3] In a simplified way, the process of $CaCO_3$ formation and dissolution, or inorganic carbon metabolism, can be illustrated as

$$Ca^{2+} + 2HCO_3^- \leftrightarrow CaCO_3 + CO_2 + H_2O \quad (1)$$

When 1 mole of $CaCO_3$ is produced or dissolved, the corresponding variations of dissolved calcium ions (Ca^{2+}) and total alkalinity (TAlk) are 1 and 2 moles, respectively. Therefore, both Ca^{2+} and TAlk are used to study $CaCO_3$ production and/or dissolution in the ocean. Ca^{2+}, one of the eleven major ions in seawater, has been recognized for a long time to be nonconservative in the ocean [*Millero*, 2006; *Pilson*, 1998]. The observed low ratios of calcium to chlorinity or salinity (Ca^{2+}/Cl or Ca^{2+}/Sal ratio) in the surface water remain an outstanding question. Prior to early 1970s, studies indicated that the surface low ratios were due to calcareous shell construction via biotic Ca^{2+} uptake, and elevated ratios in deep waters were caused by increasing solubility and carbonate dissolution owing to higher pressure, lower temperature and increasing CO_2 loading [*Dittmar*, 1884; *Culkin and Cox*, 1966; *Riley and Tongudai*, 1967; *Tsunogai et al.*, 1968; *Sagi*, 1969; *Tsunogai et al.*, 1971, 1973]. Latter on, the proton flux associated with nutrients release during organic matter decomposition was appreciated to contribute to the titration of seawater TAlk [*Brewer and Goldman*, 1976], which implies that changes in the observed TAlk within a water mass will underestimate the amount of $CaCO_3$ dissolved; thus, the "potential alkalinity" (PTA) was introduced to assess the Ca^{2+}-TAlk relationship via proton correction, which can be expressed

[1]State Key Laboratory of Marine Environmental Science, College of Oceanography and Environmental Science, Xiamen University, Xiamen, China.

0886-6236/11/2009GB003690

as $\Delta PTA = \Delta TAlk + \Delta NO_3 + \Delta PO_4$ (Δ denotes the difference between two water masses) [*Brewer et al.*, 1975].

[4] Unlike TAlk, which is affected by both organic and inorganic carbon production/consumption, the variations of Ca^{2+} in the ocean interior are almost solely controlled by $CaCO_3$ formation and dissolution on day-to-decade time scales. The advantage of using Ca^{2+} to look into the marine $CaCO_3$ cycle is thus obvious. However, reports of Ca^{2+} distribution are less popular since the change in seawater Ca^{2+} is relatively small, typically representing only ~1% of its ambient concentration (~10,280 μmol kg^{-1} at a salinity of 35 [*Pilson*, 1998]). Alternatively, abundant studies tend to provide high-quality TAlk data, which forms a strong knowledge base of present estimates of oceanic $CaCO_3$ production, export, and dissolution (see the review by *Berelson et al.* [2007]).

[5] Lysocline is defined as the depth in the water column where a critical undersaturation state with respect to aragonite or calcite results in a distinct increase in the $CaCO_3$ dissolution rate [*Morse*, 1974]. The majority of $CaCO_3$ dissolution is thus believed to occur only below the depth of the lysocline, typically below 1000 m. However, *Milliman et al.* [1999] proposed the concept of supralysocline dissolution. This concept of shallow-depth $CaCO_3$ dissolution above the lysocline contradicts the conventional understanding and provides a new vision on the marine $CaCO_3$ cycle. At A Long-Term Oligotrophic Habitat Assessment (ALOHA) Station in the North Pacific, *Milliman et al.* [1999] revealed that a significant fraction as high as 60–80 μmol kg^{-1} of Ca^{2+} was in excess above the aragonite lysocline, defined as the difference between measured Ca^{2+} ($Ca^{2+}\_^{meas}$) and Ca^{2+} calculated from a conservative Ca^{2+}/Sal ratio. Considering the preformed value which is the Ca^{2+} content in the preformed water from the Southern Ocean to the North Pacific, however, *Chen* [2002] pointed out that this excess was reduced to only 10 μmol kg^{-1}, which was not much larger than the analytical uncertainty level. Thus, when using Ca^{2+} to evaluate in situ $CaCO_3$ dissolution for a given water mass, the influence from its preformed water must be removed and the choice of reasonable preformed values becomes tricky.

[6] On the other hand, *Berelson et al.* [2007] summarized the $CaCO_3$ dissolution flux estimates via examining TAlk patterns of major oceans. The total dissolution flux in upper 200–1500 m of the world ocean was estimated to be ~1.0 Gt $CaCO_3$ yr^{-1}, which is ~2.5 times higher than that below 2000 m. As a consequence, *Berelson et al.* [2007] concluded that dissolution of settling carbonate particles should occur to a greater extent in the upper water column where waters are mostly oversaturated with $CaCO_3$. However, *Friis et al.* [2006, 2007] suggested possible overestimation of shallow-depth $CaCO_3$ dissolution, also using the TAlk evaluation. The TAlk approach usually employs a TA* term, which denotes the excess TAlk and is obtained by subtracting the preformed TAlk value from the observed one and calibrating changes induced by the protons flux [see *Feely et al.*, 2002, equation 5]. And the assumption for using TA* to estimate the $CaCO_3$ dissolution flux is that the only source of TA* in seawater is $CaCO_3$ dissolution. This approach should be applied with further caution, because additional processes such as denitrification that are apparently unrelated to $CaCO_3$ dissolution can also contribute to TA* [*Chen*, 2002; *Wolf-Gladrow et al.*, 2007]. Studies have also shown that TAlk measurements are subject to interferences from dissolved organic bases, which might add additional complications in the TAlk application [*Hernández-Ayon et al.*, 2007; *Kim and Lee*, 2009]. Ca^{2+} does not suffer from such potential issues. The excess Ca^{2+} ($Ca^{2+}\_^{ex}$) in the ocean interior, if it exists, can only have originated from $CaCO_3$ dissolution, especially in waters at shallow depth being hardly influenced by hydrothermal inputs [*de Villiers and Nelson*, 1999]. There is conjecture that dissolution or ion change of silicate material in the water might increase Ca^{2+} in the intermediate water [*Tsunogai et al.*, 1973], however, until now there is no report of such processes.

[7] While we also recognize the potential of shallow-depth $CaCO_3$ dissolution from many trap studies [e.g., *Martin et al.*, 1993; *Honjo et al.*, 1995; *Wong et al.*, 1999], the magnitude and the causes accounting for shallow-depth $CaCO_3$ dissolution warrant further examination, in particular in the context of better predicting the response of oceanic buffer capacity to increasing penetrated anthropogenic CO_2. We argue that high-quality Ca^{2+} data from a proper study site with distinguishable preformed waters are required to better examine this shallow-depth $CaCO_3$ dynamics.

[8] The South China Sea (SCS) holds an only source of deep water from the adjacent West Philippine Sea (WPS) and the water residence time in the SCS is also well studied [*Chen et al.*, 2001; *Qu et al.*, 2006]. This unique circulation pattern provides us a unique opportunity to explore the potentially different Ca^{2+} behavior between the two seas with the WPS as the preformed water mass, and subsequently to estimate the $CaCO_3$ dissolution rate. Note that previous studies have suggested that marginal seas can significantly contribute Ca^{2+} and TAlk exports to the pelagic ocean [*Milliman*, 1993; *Milliman and Droxler*, 1996]. Our study in the SCS, the largest marginal sea in the western North Pacific, aims to further explore such processes associated with marginal sea–open ocean interactions.

2. Material and Methods

2.1. The Study Area

[9] With a total area of 3.5×10^6 km^2, the SCS is the world's largest tropical-subtropical marginal sea. The East Asian Monsoon prevails in the SCS, resulting in a seasonal reversal in surface circulation with a cyclonic gyre in the winter and an anticyclonic gyre during the summer (Figure 1). Due to input from some of the major world rivers (e.g., the Mekong River and the Pearl River; see Figure 1) and influence by intensive upwelling, internal waves, and strong mixing [*Chao et al.*, 1996; *Liu et al.*, 2006], the SCS receives a large supply of nutrients to the euphotic zone, leading to a relatively higher biological productivity compared to the adjacent western North Pacific [*Liu et al.*, 2002; *Chen and Chen*, 2006]. The SCS and the western North Pacific exchange their water via the 2200 m deep Luzon Strait, through which, the Kuroshio Branch Water intrudes from the WPS into the SCS basin area (Figure 1). A "middepth front" between 350 and 1350 m, where the abrupt transition occurs between SCS and WPS proper waters, exists in the Luzon Strait near 122°E. East of this middepth front the water mass belongs to the WPS whereas the SCS water mass mostly lies to

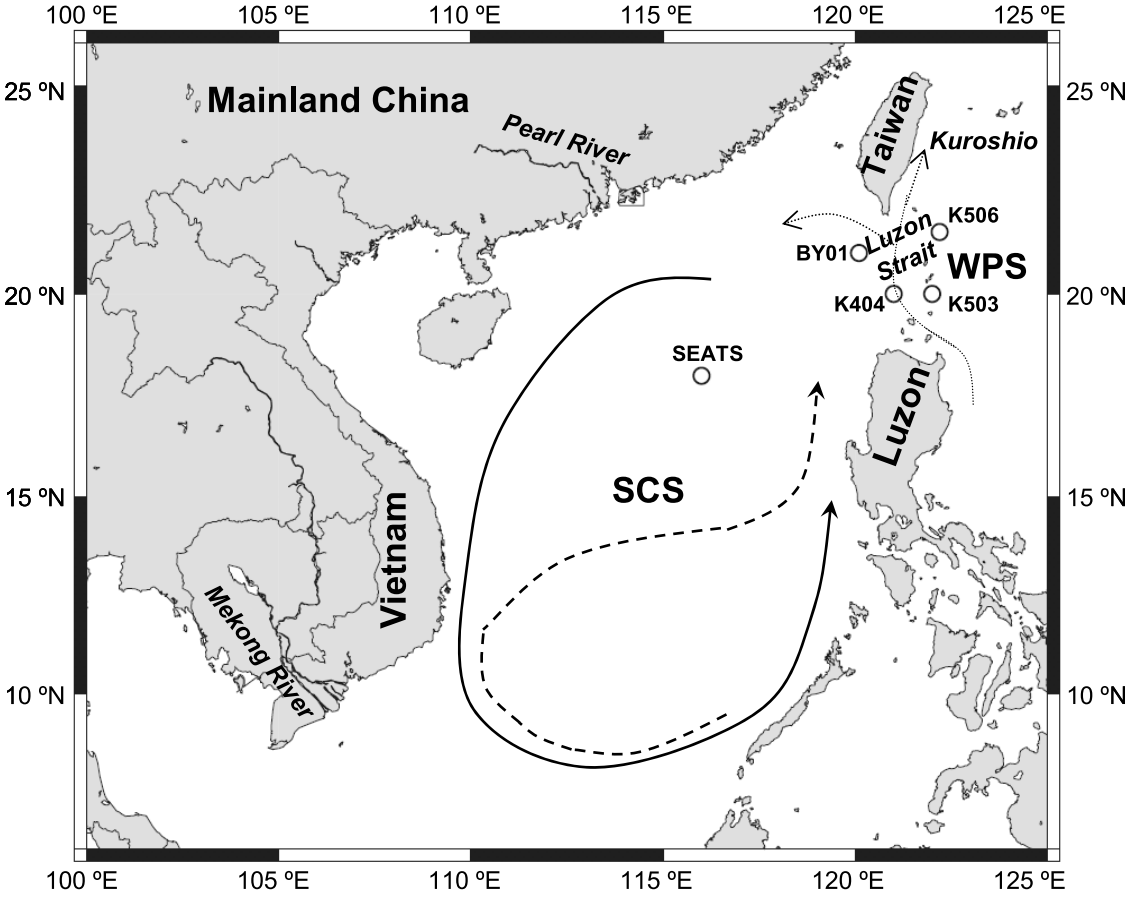

Figure 1. Map of the South China Sea showing the locations of sampling stations (SEATS: 18.0°N, 116.0°E; BY01: 21.0°N, 120.1°E; K404: 20.0°N, 121.0°E; K506: 21.5°N, 122.2°E; K503: 20.0°N, 122.0°E). The basin scale circulation pattern is according to *Wong et al.* [2007, and references therein], showing a basin wide cyclonic gyre in winter (solid line) and an anticyclonic gyre over the southern half of the South China Sea in summer (dashed line). Also shown schematically are the Kuroshio and its intrusions into the northern South China Sea around the Luzon Strait (dotted line) according to *Wong et al.* [2007, and references therein].

the west [*Chen and Huang*, 1996]. Previous studies [*Chao et al.*, 1996; *Li and Qu*, 2006; *Qu et al.*, 2006; *Tian et al.*, 2006] have indicated a "sandwich-like" structure of water exchanges across the Luzon Strait, with a net inflow from the Pacific in the surface and deep layers and a net outflow from the SCS in the intermediate layer. In terms of mass balance, the rapid replenishment of the SCS deep water from the WPS is maintained by fast ventilation with the shallower intermediate water, as well as a persistent net outflow at an intermediate depth [*Chao et al.*, 1996; *Chen et al.*, 2006; *Li and Qu*, 2006]. This unique flow pattern therefore provides an opportunity to study both the material exchange across different depths between the two seas and the independent biogeochemical processes in the SCS relative to the WPS [*Dai et al.*, 2009].

2.2. Sampling and Analyses

[10] Seawater samples were collected in September 2007 at the South East Asian Time-series Study (SEATS) station established in the SCS basin on board R/V *Dongfanghong II* and in September 2008 at stations BY01, K404, K503, and K506 on board R/V *Shiyan III*. K503 and K506 were located right on the middepth front, and other stations were located to its west at different distances (Figure 1). Water column samples were collected with Niskin bottles attached on a Rosette sampler. Samples for Ca^{2+} analysis were stored in 60 mL acid-cleaned polyethylene bottles with Parafilm wrapped around the cap. Samples for TAlk and dissolved inorganic carbon (DIC) analysis were stored in 100 mL polyethylene bottles and 40 mL borosilicate glass Environmental Protection Agency (EPA) vials, respectively. Both TAlk and DIC samples were poisoned with $HgCl_2$-saturated solution upon sample collection, with 100 μL for TAlk and 50 μL for DIC.

[11] In the laboratory, Ca^{2+} was determined using the classic ethylene glycol tetraacetic acid (EGTA) titration modified from *Lebel and Poisson* [1976]. About 4 g of seawater and 4 g of $HgCl_2$ solution (~1 mmol L^{-1}) were accurately weighed out; then about 4 g of a concentrated EGTA solution (~10 mmol L^{-1}, also by weighing) was added to complex Hg^{2+} completely and nearly 95% of Ca^{2+}. After adding 4 mL of borate buffer, the remaining

Ca^{2+} was titrated by a diluted solution of EGTA (~2 mmol L^{-1}) up to the end point potential, which was given by the Methrom 809 TITRANDO potentiometer with an amalgamated silver combined electrode (Methrom Ag Titrode). Instead of using the autogenerated value given by the Methrom TiAMO 1.1 software, the volume of the diluted solution of EGTA necessary for the remaining ~5% of Ca^{2+} was obtained by manually fitting the first derivative of the titration curve, which proved to be optimal for better measurement precision (10,006 ± 95 μmol kg^{-1} versus 10,190 ± 6 μmol kg^{-1}, 1σ, n = 24; the latter method yielded a precision of ~0.06%). EGTA solutions were standardized daily against International Association for the Physical Sciences of the Oceans (IAPSO) standard seawater (Batch P147, Salinity = 34.993). Standard seawater of the same batch was calibrated against a standard Ca^{2+} solution in a synthetic seawater matrix. The Ca^{2+}/Sal ratio of Batch P147 was determined to be 292.3, which is higher than that of Batch P61 (291.3 [*Shiller and Gieskes*, 1980]) and Batch P79 (290.5 [*Olson and Chen*, 1982]), but lower than Batch P67 (293.0 [*Kanamori and Ikegami*, 1980]). The reasons causing the variations of the Ca^{2+}/Sal ratio among different batches of IAPSO standard seawater are unclear but could be related to the different analytical methods of Ca^{2+} analysis used by the different investigators. Alternatively, there might be small variations in Ca^{2+} in the IAPSO standard seawater because they are prepared on the basis of Atlantic Ocean surface seawater. Note that our replicated analysis did not show measurable difference between filtered and unfiltered samples within the limit of the precision. Data reported here were from unfiltered samples.

[12] DIC was determined by acidification of 0.5 mL of a water sample and the subsequent quantification of CO_2 with a nondispersive IR detector (Li-Cor 7000). This method has a precision of 0.1% [*Cai et al.*, 2004]. TAlk was determined by Gran titration on a 25 mL sample with a Kloehn digital syringe pump, with a precision of 2 μmol kg^{-1}. Both DIC and TAlk were calibrated against the certified reference material provided by Dr. A. Dickson of the Scripps Institution of Oceanography. Depth profiles of temperature and salinity were determined shipboard with the SBE9/11 Conductivity-Temperature-Depth (CTD) recorder (Sea-Bird Co.).

2.3. Ratio of $CaCO_3$ Dissolution and Organic Carbon Decomposition

[13] During the settling of surface produced particles, both $CaCO_3$ dissolution and organic carbon decomposition contribute to the TAlk and DIC addition in deeper waters, which are fundamental to the ocean's capacity to absorb CO_2. It is, therefore, important to determine the ratio of the DIC addition between $CaCO_3$ dissolution and organic carbon decomposition (IC/OC ratio).

[14] Equations (2)–(8) have been used previously to calculate the IC/OC ratio in the Pacific Ocean and the WPS and SCS [*Chen et al.*, 1982, 2006]. In this study, TAlk, DIC and potential temperature (PT) data from station SEATS were applied to calculate the IC/OC ratio in deep waters of the SCS.

$$\mathrm{IC/OC} = [0.16038(\Delta\mathrm{DIC} + 45) + \Delta\mathrm{TAlk}] / [2(\Delta\mathrm{DIC} + 45) - \Delta\mathrm{TAlk}] \quad (2)$$

$$\Delta\mathrm{DIC}\left(\mu\mathrm{mol\,kg^{-1}}\right) = \mathrm{DIC^{meas}} - \mathrm{DIC^{\circ}} = \mathrm{DIC^{meas}} - \mathrm{NDIC^{\circ}} \times \mathrm{Sal}/35 \quad (3)$$

$$\Delta\mathrm{TAlk}\left(\mu\mathrm{mol\,kg^{-1}}\right) = \mathrm{TAlk^{meas}} - \mathrm{TAlk^{\circ}} = \mathrm{TAlk^{meas}} - \mathrm{NTAlk^{\circ}} \times \mathrm{Sal}/35 \quad (4)$$

For deep and bottom waters:

$$\mathrm{NDIC^{\circ}}\left(\mu\mathrm{mol\,kg^{-1}}\right) = 2219 - 11 \times \mathrm{PT}(\pm 16) \quad (5)$$

$$\mathrm{NTAlk^{\circ}}\left(\mu\mathrm{mol\,kg^{-1}}\right) = 2384 - 4.2 \times \mathrm{PT}(\pm 9) \quad (6)$$

For salinity minimum waters and waters above:

$$\mathrm{NDIC^{\circ}}\left(\mu\mathrm{mol\,kg^{-1}}\right) = 2242 - 12.08 \times \mathrm{PT}(\pm 18) \quad (7)$$

$$\mathrm{NTAlk^{\circ}}\left(\mu\mathrm{mol\,kg^{-1}}\right) = 2384 - 3.36 \times \mathrm{PT}(\pm 11) \quad (8)$$

The superscript "meas" and the degree symbol denote measured and preformed values, respectively, and their difference is the addition of DIC, TAlk, or Ca^{2+} and is represented as Δ. N denotes the value normalized to a salinity of 35. Sal and PT are salinity and potential temperature.

[15] Equation (2) is deduced on the basis of the stoichiometric relationship during the inorganic and organic carbon metabolism. DIC and Ca^{2+} increase by 1 mol, and TAlk increases by 2 moles per mole $CaCO_3$ dissolution (equation (1)). On the other hand, during 1 unit organic carbon decomposition the change in TAlk with increase in DIC is minor (−17 versus 106; $(CH_2O)_{106}(NH_3)_{16}H_3PO_4 + 138O_2 \leftrightarrow 106CO_2 + 122H_2O + 16HNO_3 + H_3PO_4$). Assuming that x μmoles of $CaCO_3$ dissolve and y μmoles of organic carbon decompose in 1 kg of seawater, the additions of TAlk and DIC can be written as $\Delta\mathrm{TAlk} = 2x - 17y$ and $\Delta\mathrm{DIC} = x + 106y$. After solving for x and y with ΔTAlk and ΔDIC, equation (2) can be yielded from IC/OC = $x/106y$ [*Chen et al.*, 1982]. Note that the value of 45 (μmol kg^{-1}) in equation (2) is the estimated average amount of anthropogenic CO_2 input in the SCS and the WPS by *Chen et al.* [2006] based on field data collected around 1997 with an uncertainty of ±30%. After 10 years till our sampling period, the anthropogenic CO_2 content should increase but only to a small extent when considering that the surface NDIC was predicted to ~60 μmol kg^{-1} higher in 2050 than in 1997 [*Chen et al.*, 2006]. Therefore, we still employed the value of 45 in this study, and this anthropogenic CO_2 contribution should be subtracted from DIC° to better quantify the portion originating from the $CaCO_3$ dissolution and organic carbon decomposition [*Chen et al.*, 2006].

[16] The preformed value is fixed when a given water mass was last in contact with the atmosphere and can be calculated from PT because the two properties are well correlated in a given ocean basin [*Chen and Pytkowicz*, 1979]. Equations (5)–(8) were obtained by fitting surface DIC or TAlk to PT in the North Pacific by *Chen et al.* [2006] on the basis of revised GEOSECS data (T. Takahashi et al., Carbonate chemistry of the Atlantic, Pacific, and Indian Oceans: The results of the

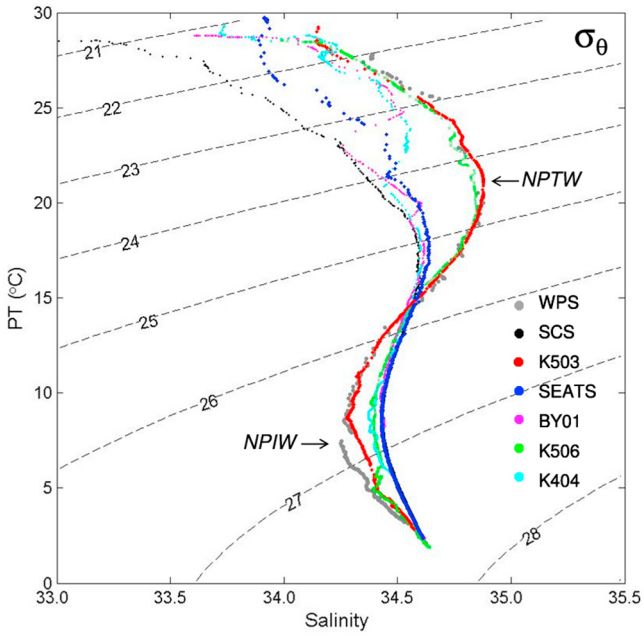

Figure 2. Potential temperature (PT) versus salinity plots (T-S diagram) for the sampling stations. Data for stations BY01, K404, K503, and K506 from the 2008 cruise were provided by D. Wang et al. (unpublished data, 2009). The South China Sea proper water data were from the 2007 cruise. The West Philippine Sea proper water data were from World Ocean Database 2005 Geographically Sorted Data (Available at http://www.nodc.noaa.gov/OC5/WOD05/docwod05.html [*Johnson et al.*, 2006]). Also indicated are the North Pacific Tropical Water (NPTW) and the North Pacific Intermediate Water (NPIW) with salinity extremes.

GEOSECS expeditions, 1972–1978, unpublished document, 1980). The numbers in parentheses give 1 standard deviation of the least squares fit.

2.4. The Addition of Ca^{2+} From $CaCO_3$ Dissolution

[17] On the basis of previous studies, the addition of Ca^{2+} (ΔCa^{2+}) from $CaCO_3$ dissolution in deep waters can be estimated on the basis of the combination of the addition of TAlk (ΔTAlk) and the addition of DIC (ΔDIC [*Chen et al.*, 1982]):

$$\text{Estimated } \Delta Ca^{2+}\left(\mu\text{mol kg}^{-1}\right) = 0.46288\Delta\text{TAlk} + 0.074236(\Delta\text{DIC} + 45) \quad (9)$$

or directly obtained from Ca^{2+_meas} subtracting the preformed Ca^{2+} value ($NCa^{2+\circ}$ [*Chen*, 2002]):

$$NCa^{2+\circ}\left(\mu\text{mol kg}^{-1}\right) = 10,240 - 3.53 \times \text{PT}(\pm 6, \text{PT} \le 20^{\circ}\text{C}) = 10,170(\pm 5, \text{PT} > 20^{\circ}\text{C}) \quad (10)$$

$$\text{Measured } \Delta Ca^{2+}\left(\mu\text{mol kg}^{-1}\right) = Ca^{2+\_meas} - Ca^{2+\circ} = Ca^{2+\_meas} - NCa^{2+\circ} \times \text{Sal}/35 \quad (11)$$

[18] Equation (9) is also deduced on the basis of the stoichiometric relationship during the inorganic and organic carbon metabolism. The estimated ΔCa^{2+} equals x which has been solved during the deduction of equation (2) [*Chen et al.*, 1982]. In this study, we added the value of 45 (μmol kg^{-1}) for calibrating the anthropogenic CO_2 input.

[19] Equation (10) was obtained by fitting surface Ca^{2+} to PT by *Chen* [2002] on the basis of the combined data of the Pacific Ocean [*Tsunogai et al.*, 1973] and the Weddell Sea [*Chen*, 1983]. The numbers in parentheses give 1 standard deviation of the least squares fit.

[20] In this study, both estimated ΔCa^{2+} and measured ΔCa^{2+} were obtained from the deep water at station SEATS.

3. Results

3.1. Hydrography

[21] As shown in the Temperature-Salinity (T-S) diagram (Figure 2), all surface waters collected during the present study (PT > 25°C, top 100 m) were mixtures of SCS and WPS proper waters with varied combinations of both. The lower surface salinity in the SCS interior is attributed to the basin-wide net precipitation and large river input (i.e., the Pearl River). At the subsurface, the T-S distribution pattern at station K503 was mostly reflective of WPS proper waters, whereas at stations SEATS and BY01 it showed characteristics of SCS proper waters. The observed patterns for T-S distribution at stations K506 and K404 represented a mixture of SCS and WPS waters with a higher contribution from the SCS. Both the salinity maximum and minimum could still be found at station SEATS, less pronounced though as compared to station K503. These salinity extremes in the SCS and the WPS are influenced by the North Pacific Tropical Water (NPTW) and the North Pacific Intermediate Water (NPIW) sourced from the subpolar region, respectively [*Dai et al.*, 2009, and references therein], whereas the intensive upwelling and vertical mixing in the SCS interior must have reduced those extreme signals [*Chen et al.*, 2006]. The overall SCS water T-S property, therefore, showed a less curved inverse S shape as compared to that of the WPS (Figure 2).

3.2. Vertical Ca^{2+} Distribution

[22] The Ca^{2+} distribution largely followed the salinity (Figure 3). At station SEATS in the inner basin of the SCS, Ca^{2+} increased considerably from surface to up to 150 m coinciding with the zone of shallow salinity maximum layer at a density level (σ_θ) of ~25.5. Below 150 m, Ca^{2+} concentrations showed a sharp decrease until the intermediate salinity minimum layer at a depth of ~450 m with σ_θ ~ 26.5–27.0. Below 500 m, Ca^{2+} concentration increased again until it reached an almost constant value in the bottom water (>1500 m, σ_θ > 27.5). The Ca^{2+}/Sal ratio in the top 100 m water at station SEATS was constant. It increased rapidly from 200 m to up to 800 m and showed a slight increase below 800 m (Figure 3). The average Ca^{2+}/Sal ratios in the subsurface (200–800 m) and deep waters (below 1000 m) were ~0.3% and ~0.7% higher than that of the top 100 m water, corresponding to an additional Ca^{2+} content of ~31 and ~72 μmol kg^{-1}, respectively.

[23] The values of surface salinity and Ca^{2+} from stations K503 and K506 were significantly higher than those of stations BY01 and K404 (Figure 3), suggesting the dilution by fresh water input at the latter two stations in the SCS

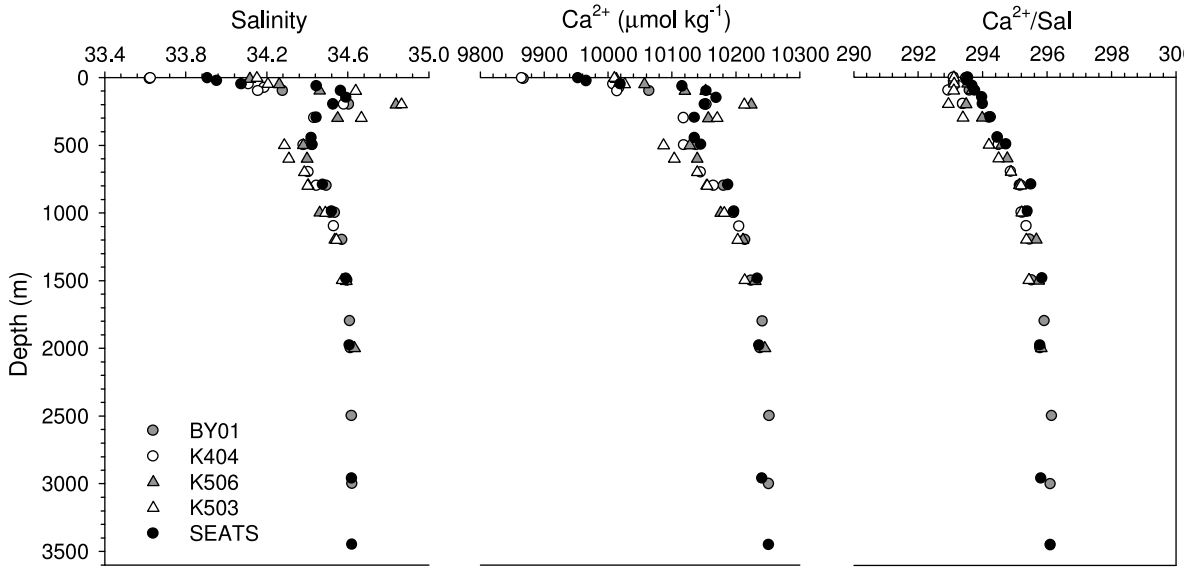

Figure 3. Vertical distribution of salinity, Ca^{2+}, and Ca^{2+}/Sal ratio at the sampling stations. Salinity data for stations BY01, K404, K503, and K506 were provided by D. Wang et al. (unpublished data, 2009).

interior. Around the 200 m depth (the shallow salinity maximum layer of the WPS at $\sigma_\theta \sim 24.5$), K503 and K506 also displayed much higher salinity and Ca^{2+} values, indicating the relatively strong influence of the NPTW on these two sites located at the middepth front. However, the observed salinity and Ca^{2+} at the intermediate salinity minimum layer at K503 (~500 m, $\sigma_\theta \sim 26.5$) were lower, whereas in the case of K506 these values were much closer to those of BY01 and K404, indicating the possible influence of the intermediate SCS outflow waters on the station K506. Below the depth of ~1000 m ($\sigma_\theta > 27.3$), there was no noticeable difference in the content of salinity and Ca^{2+} among the four study stations primarily due to the rapid renewal of the SCS deep water.

[24] In the surface layer (top 100 m), Ca^{2+}/Sal ratios were higher at stations BY01 and K506 than K503 and K404. At the depth between 200 and 600 m, the Ca^{2+}/Sal ratio of K503 was remarkably lower, whereas below 600 m, no apparent difference was observed in Ca^{2+}/Sal ratios. The surface Ca^{2+}/Sal ratios of K404 were more similar to K503 than BY01 located in the west of the front (Figure 3). The reason for this discrepancy is unclear, but possibly due to the fact that K404 is located in the slope area (with a water depth of 1250 m) under dynamic environmental settings. Some local processes such as mixing with other end-members or strong biouptake of Ca^{2+} might lower the surface Ca^{2+}/Sal ratios. This might be also true in the case of K503 and K506, where the water depth of K503 (1990 m) is much shallower than that of K506 (4650 m).

4. Discussion

4.1. Excess Ca^{2+} in the SCS Subsurface Water and Shallow-Depth $CaCO_3$ Dissolution

[25] The T-S property patterns (Figure 2) suggest that in the subsurface and intermediate layers, the hydrographic characteristic of the SCS waters (i.e., SEATS) were very different from those of the WPS waters (i.e., K503). A closer look at the PT and Ca^{2+} profiles at stations SEATS and K503 (Figure 4) revealed that the subsurface water (200–800 m) of the SCS was relatively cold and Ca^{2+} enriched. The relatively higher Ca^{2+} in the SCS than the WPS might be a consequence of the in situ $CaCO_3$ dissolution and/or upwelled Ca^{2+}-rich deeper waters in the SCS interior.

[26] To distinguish the two potential processes leading to the higher Ca^{2+} in the SCS, we first constructed the relationship between Ca^{2+} and PT for the K503 waters between 200 and 1000 m as PT is conservative during the transport of a given water mass (Figure 5a). We then substituted the measured PT of the SEATS subsurface water into the above relationship to obtain their preformed Ca^{2+} value (denoted as $Ca^{2+}_{\_pre}$ to distinguish itself from the term $NCa^{2+\circ}$ in equations (10) and (11)) produced via physical processes such as upwelling and vertical mixing in the SCS interior. As a consequence, $Ca^{2+}_{\_ex}$ was the difference between $Ca^{2+}_{\_meas}$ and $Ca^{2+}_{\_pre}$, which signifies the amount of Ca^{2+} enriched through $CaCO_3$ dissolution (Figure 5b). As shown, Ca^{2+} remained higher in the subsurface layer (corresponding to the PT range from ~5 to 20°C) at SEATS than at K503 (Figure 5a). The average concentration of $Ca^{2+}_{\_ex}$ in the subsurface waters at 200–800 m at SEATS was estimated to be 13 ± 5 μmol kg^{-1} (Figure 5b). It is reasonable to argue that it is impossible for processes such as hydrothermal input to affect the Ca^{2+} behavior within this depth range of the SCS. The significant amount of $Ca^{2+}_{\_ex}$ found in the SCS thus should be reflective of Ca^{2+} additions from the dissolution of sinking carbonate particles produced in the surface layer of the SCS. The total additional Ca^{2+} content in the SCS subsurface water relative to the local top 100 m water was ~31 μmol kg^{-1}. In this context, almost 40% (approximate 13/31) of the increased Ca^{2+} was due to in situ $CaCO_3$ dissolution with the remainder 60% (approximate (31 − 13)/31) coming from the upwelled Ca^{2+}-rich deeper waters.

[27] With the residence time of ~50 years for the SCS intermediate water [*Chen et al.*, 2001], we obtained a

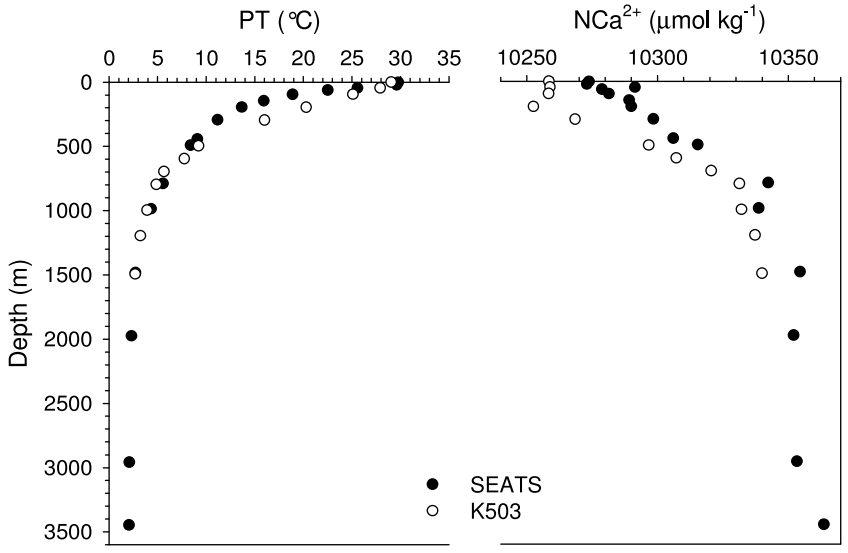

Figure 4. Depth distribution of PT and Ca^{2+} (normalized to a salinity of 35) of seawater samples collected at stations SEATS and K503. PT data for station K503 were provided by D. Wang et al. (unpublished data, 2009).

$CaCO_3$ dissolution rate of ~0.5 mmol m^{-2} d^{-1} in the waters at 200–800 m, which is similar to the range of dissolution rates in the Pacific shallow depth [see *Feely et al.*, 2002, Table 1] and is close to the average $CaCO_3$ lost between two traps deployed at 124 and 620 m, respectively, in the SCS basin (station KK3: 18.3°N, 115.7°E [*Cai*, 2007]). Direct reports on the $CaCO_3$ export flux of the SCS basin are scarce. However, the global $CaCO_3$ export flux estimated from models is 0.3–1.1 mmol m^{-2} d^{-1} [*Berelson et al.*, 2007]. Thus, it is reasonable to contend that more than half of biogenic $CaCO_3$ particles escaped from the euphotic zone would dissolve in the SCS upper 1000 m water columns, which coincides with the anthropogenic CO_2 penetration depth in the SCS [*Chen et al.*, 2006]. $CaCO_3$ dissolution above this depth would convert this CO_2 to HCO_3^- (equation (1)), thereby further stimulating the onsite oceanic uptake of CO_2.

[28] Due to the fact that waters between 200 and 800 m in the SCS are mostly oversaturated with respect to both aragonite and calcite [*Chen et al.*, 2006], it is impossible that the thermodynamically predicted $CaCO_3$ dissolution at depths below the lysocline leads to the $Ca^{2+}\_^{ex}$. Together with the significant DIC increase in the similar water depth range (DIC^{bio} between 100 and 600 m [*Chou et al.*, 2007; *Sheu et al.*, 2009]), the $Ca^{2+}\_^{ex}$ observed in the SCS subsurface water may support the second "possible mechanism"

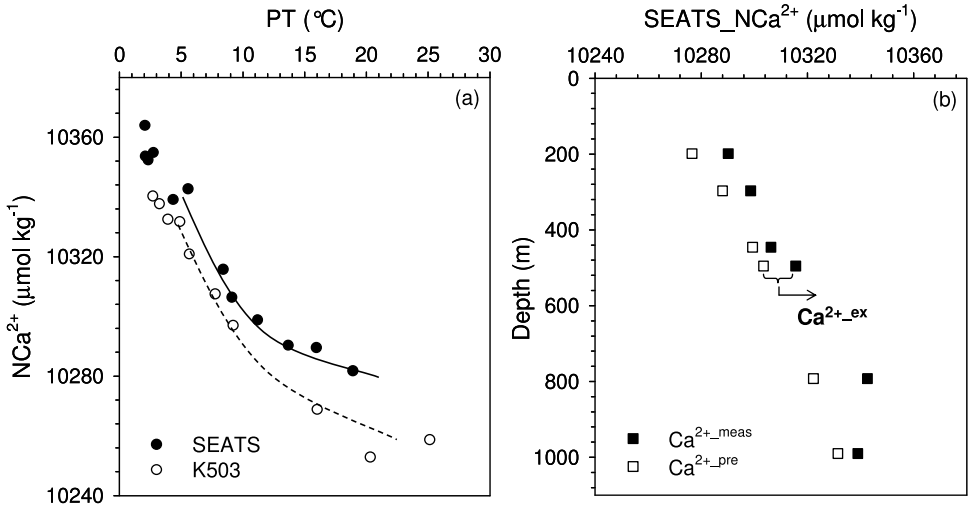

Figure 5. (a) Ca^{2+} versus PT below the depth of 100 m for stations SEATS and K503. For the K503 waters between 200 and 1000 m, the relationship was given by the equation $NCa^{2+} = (10210 \pm 2) + (161.0 \pm 5.6) \times \exp[-PT/(15.5 \pm 0.5)]$, $r = 0.99$. PT data for station K503 were provided by D. Wang et al. (unpublished data, 2009). (b) Depth profiles of measured Ca^{2+} ($Ca^{2+}\_^{meas}$) and preformed Ca^{2+} ($Ca^{2+}\_^{pre}$) from 200 to 1000 m for station SEATS. All Ca^{2+} data were normalized to a salinity of 35.

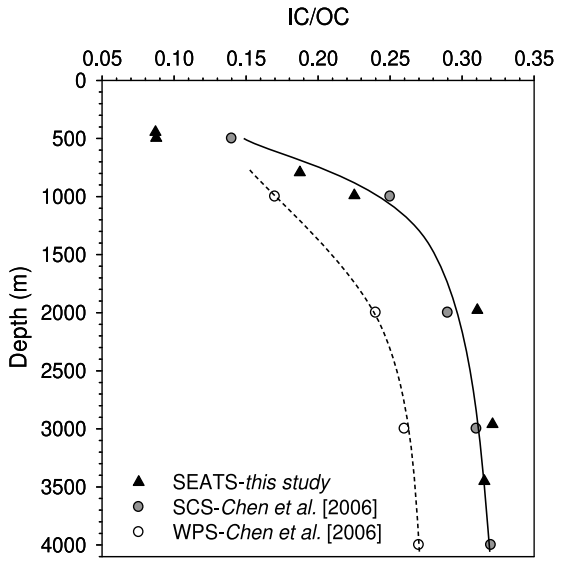

Figure 6. Ratios of the DIC addition between $CaCO_3$ dissolution and organic carbon decomposition (IC/OC ratios) below 500 m at station SEATS. Also shown are the IC/OC ratios in the South China Sea and West Philippine Sea obtained by *Chen et al.* [2006].

envisioned by *Milliman et al.* [1999], i.e., supralysocline dissolution due to the microbial oxidation of organic matter that produces a microenvironment conducive to carbonate dissolution. *Wollast and Chou* [1998, 2001] also demonstrated that shallow-depth $CaCO_3$ dissolution could happen in oversaturated waters in the Gulf of Biscay, and proposed that the "microenvironment" might be the interior of fecal pellets or the surface of biogenic aragonite or calcite. Through examining Mg/Ca ratio in the shell of planktonic foraminifers at four water depths, *Huang et al.* [2008] proposed partial dissolution at depths well above the calcite lysocline in the SCS. In this study, by straightly analyzing seawater Ca^{2+}, we demonstrated that shallow-depth $CaCO_3$ dissolution does occur in the SCS.

[29] Moreover, other investigators have suggested $CaCO_3$ dissolution in the euphotic zone. *Moore et al.* [2002, 2004] proposed models showing that 30%–50% of the $CaCO_3$ produced in surface waters would dissolve before escaping the euphotic zone. By estimating the weight of coccoliths from two sediment traps deployed at the same tropical Atlantic site, but separated by 2000 m water depth, *Beaufort et al.* [2007] found no significant coccolith dissolution during settling between 250 and 2500 m, but proposed that most of the dissolution occurs in the euphotic zone and possibly in the guts of grazers. In this study, although normalized Ca^{2+} concentrations were higher in the top 100 m waters at SEATS than at K503 (Figure 4), whether $CaCO_3$ was dissolved in the euphotic zone of the SCS is not certain because the signature of normalized Ca^{2+} (against a salinity of 35) may well be compounded by the riverine Ca^{2+} input.

4.2. Ca^{2+} Export Out of the SCS Through Shallow-Depth $CaCO_3$ Dissolution

[30] With an annual outflow of 1.9 ± 0.4 Sv for the SCS subsurface waters [*Chen et al.*, 2001; *Chou et al.*, 2007; *Sheu et al.*, 2009] and the average $Ca^{2+}{}_{-ex}$ concentration of 13 ± 5 μmol kg^{-1}, we estimated that the SCS subsurface outflow would export (0.8 ± 0.3) × 10^{12} mol yr^{-1} of Ca^{2+} out of the SCS. This flux is ~10% of the global annual input of Ca^{2+} from the marginal sea to the open oceans [*Milliman*, 1993; *Milliman and Droxler*, 1996] and represents the Ca^{2+} and TAlk additions from the water column dissolution in the continental margins. Moreover, along with the northwardly flowing Kuroshio Current (Figure 1), the Ca^{2+}/TAlk-laden SCS subsurface water would travel to high-latitude region in the western North Pacific, even upwell onto the East China Sea (ECS) [*Chen*, 1996], which is finally conducive to the CO_2 uptake of waters around the Kuroshio regime.

[31] Thus far, it is believed that the ocean margin contribution of TAlk to the open ocean is mainly related to the processes occurring in the ocean margin sediments [*Chen*, 2002; *Berelson et al.*, 2007]. Both benthic carbonate dissolution and anaerobic processes such as sulfate reduction involving precipitation of iron sulfides [*Hammond et al.*, 1999] and denitrification [*Fennel et al.*, 2008; *Thomas et al.*, 2009] generate TAlk, which might be transported horizontally to contribute to TA* in the upper water column of the open ocean. Our results indicated, for the first time, that along with benthic processes, $CaCO_3$ dissolution in waters at shallow depth in marginal seas might also contribute to the TA* in the upper layer of the open ocean.

4.3. IC/OC Ratio and ΔCa^{2+} in the SCS Deep Water

[32] Due to the rapid renewal of the SCS deep water, water properties in the SCS deep layer are almost homogenous to those of the WPS [*Chou et al.*, 2007]; thus, deep waters of the SCS and the WPS have the same precursor as the Pacific Ocean, i.e., waters from the Southern Ocean. At station SEATS (Figure 6), the IC/OC ratio increased rapidly from 500 m to 2000 m, indicating the relatively high decomposition rates of organic matter in the upper water. Below 2000 m, the IC/OC ratio agreed well with the value of the SCS estimated by *Chen et al.* [2006], showing a constant value at 0.31. The IC/OC ratios of the WPS [*Chen et al.*, 2006] are lower than those of the SCS in the waters below 1000 m (Figure 6), suggesting that the deep SCS water is more corrosive and more $CaCO_3$ has been dissolved. Taking 0.29 as the average IC/OC ratio for the water below 1000 m, we estimated that during the water transport from the Southern Ocean, $CaCO_3$ dissolution contributed approximately 22% of the DIC accumulation in the deep SCS. This percentage is close to that for the deep North Pacific (~26%, IC/OC = 0.35 [*Chen*, 1990]), and both of them are higher than in the deep South Pacific (~12%, IC/OC = 0.135 [*Chen et al.*, 1982]).

[33] As shown in Figure 7, the value of the estimated ΔCa^{2+} increased with depth below 500 m at station SEATS, reached a plateau of ~45 μmol kg^{-1} at 2000 m and then remained relatively constant below 2000 m. Although the pattern looked similar for the measured ΔCa^{2+}, their values were much higher. Note that the observed additional Ca^{2+} content below 1000 m at SEATS was ~72 μmol kg^{-1}, relative to the local top 100 m water. It is unlikely that the ΔCa^{2+} level would be above this value, suggesting that our estimated ΔCa^{2+} were reasonable. We contend that the exceptional higher ΔCa^{2+} measured was mainly due to the systematic deviation of our measured Ca^{2+} from $NCa^{2+}{}^{\circ}$ (equation (10)), which is summarized from Ca^{2+} determined

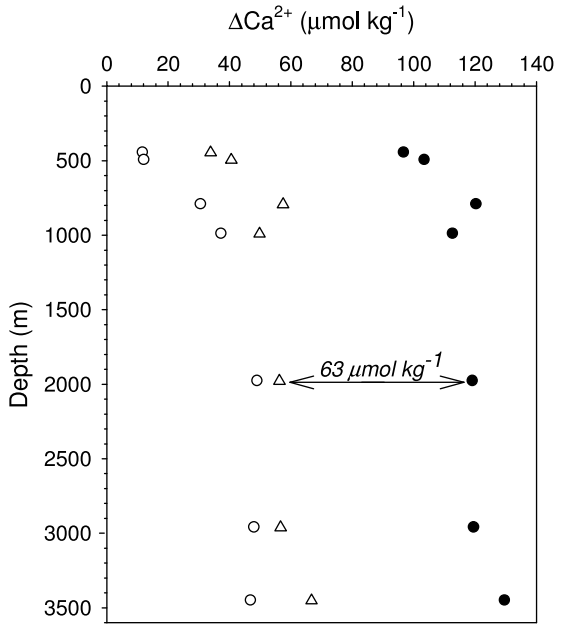

Figure 7. The addition of Ca^{2+} (ΔCa^{2+}) estimated (open circles) by equation (9) and measured (closed circles) below 500 m at station SEATS. Open triangles indicate values after subtracting 63 μmol kg^{-1} from measured ΔCa^{2+}.

using other methods [*Tsunogai et al.*, 1973; *Chen*, 1983]. In fact, the difference of the Ca^{2+} concentration of the IAPSO standard seawater measured by us and by *Olson and Chen* [1982], respectively, is 63 μmol kg^{-1} (10,230 μmol kg^{-1} for Batch P147 and 10,167 μmol kg^{-1} for Batch P79). If our measured Ca^{2+} data were shifted down by 63 μmol kg^{-1}, the difference between the estimated and measured values would be reduced to ~10–20 μmol kg^{-1} (Figure 7). Therefore, the average ΔCa^{2+} value of 51 ± 8 μmol kg^{-1} below 1000 m at the SEATS station reflected the real $CaCO_3$ flux during the journey of the deep waters from the Southern Ocean to the SCS, which is comparable to the amount of ΔNCa^{2+} (36 ± 6 μmol kg^{-1}) in the deep North Pacific Ocean relative to the Weddell Sea [*Chen*, 1990].

4.4. Ca^{2+} Versus TAlk in the Estimates of $CaCO_3$ Dissolution

[34] In waters below 100 m where $CaCO_3$ dissolves in the SCS (Figure 8), the slope of the linear regression line of Ca^{2+} to TAlk was 0.54 ± 0.03, slightly higher than the theoretical value of 0.5. Considering the effect of proton flux, the slope of the linear regression line fitted to Ca^{2+} and PTA was 0.46 ± 0.03, slightly lower than 0.5. Both of these slopes agreed well with the theoretical value within the limit of uncertainties, suggesting that Ca^{2+} and TAlk variations from subsurface to deep waters in the SCS are overall controlled by $CaCO_3$ dissolution. We note that dissolution of magnesium (Mg) calcites (in the form of $Ca_{(1-x)}Mg_xCO_3$) also releases Ca^{2+} and TAlk [*Andersson et al.*, 2007, equation 5], which could represent another potential mechanism inducing supralysocline dissolution [*Millero*, 2007]. However, the Ca^{2+}/TAlk change ratio during Mg calcites dissolution should always be <0.5 with variations dependent upon different Mg content therein. Our data with Ca^{2+} to TAlk ratio of >0.5 thus suggested that the influence of Mg calcites dissolution on Ca^{2+} should be negligible in the SCS.

[35] Elsewhere in the North Pacific [*Kanamori and Ikegami*, 1982; *Ikegami and Kanamori*, 1983], a comprehensive data set also displayed a good positive linear relationship between Ca^{2+} and TAlk throughout the whole water column (Ca^{2+} = (0.69 ± 0.02)TAlk + (8609 ± 39), r = 0.98, n = 86; Ca^{2+} = (0.54 ± 0.01)PTA + (8963 ± 24), r = 0.98, n = 86. All of the data were normalized to a salinity of 35), which could also be simply interpreted as the $CaCO_3$ formation and dissolution.

[36] Besides qualitative analysis of Ca^{2+}-TAlk relationship within water column, quantitative evidence can be obtained by evaluating $Ca^{2+}{}_{-ex}$ and excess PTA (PTA^{ex}) independently through point-by-point calculations. For example, on the basis of the preformed value obtained by *de Villiers* [1998] and data available from other investigations, she demonstrated that in deep waters close to mid-ocean ridges, $Ca^{2+}{}_{-ex}$ values were greater than the expected values for corresponding changes in PTA during $CaCO_3$ dissolution (i.e., $Ca^{2+}{}_{-ex} > 0.5PTA^{ex}$), and proposed that the mid-depth excess Ca^{2+} was supplied by hydrothermal input.

[37] In this study, by applying the same calculation method as $Ca^{2+}{}_{-ex}$, we estimated PTA^{ex} in the subsurface water at SEATS relative to K503. There was no correlation at all between $Ca^{2+}{}_{-ex}$ and PTA^{ex}, and $Ca^{2+}{}_{-ex}$ was overall higher than half of PTA^{ex} (Figure 9b). The average value of PTA^{ex} between 200 and 800 m was nearly the same as $Ca^{2+}{}_{-ex}$ (10 ± 5 μmol kg^{-1} versus 13 ± 5 μmol kg^{-1}), rather than twofold higher as expected from the good positive linear relationship between Ca^{2+} and TAlk (Figure 9a). As $Ca^{2+}{}_{-ex}$ in the SCS subsurface water could only originate from $CaCO_3$ dissolution, the discrepancy of $Ca^{2+}{}_{-ex} > 0.5PTA^{ex}$ in this study might imply the TAlk removal through other processes which have no influence on Ca^{2+} variations, and the removal content should be too minor to deteriorate the

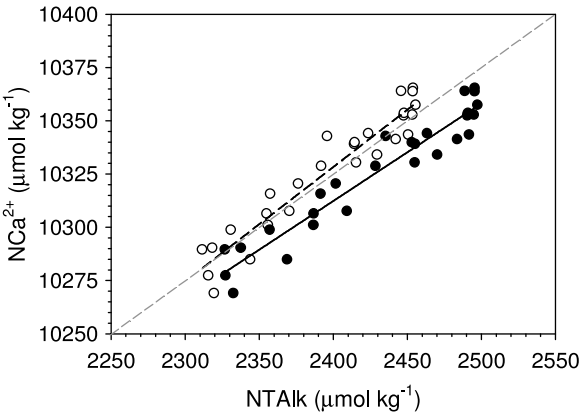

Figure 8. Ca^{2+} versus TAlk (open circles) or PTA (solid circles; PTA = TAlk + NO_3 + PO_4) in waters below 100 m at stations SEATS, K404, and BY01 in the South China Sea. Ca^{2+} = (0.54 ± 0.03)TAlk + (9038 ± 77), r = 0.96, n = 27; Ca^{2+} = (0.46 ± 0.03)PTA + (9214 ± 64), r = 0.96, n = 27. All of the data were normalized to a salinity of 35. The slope of the gray dashed line is equal to the theoretical value of 0.5.

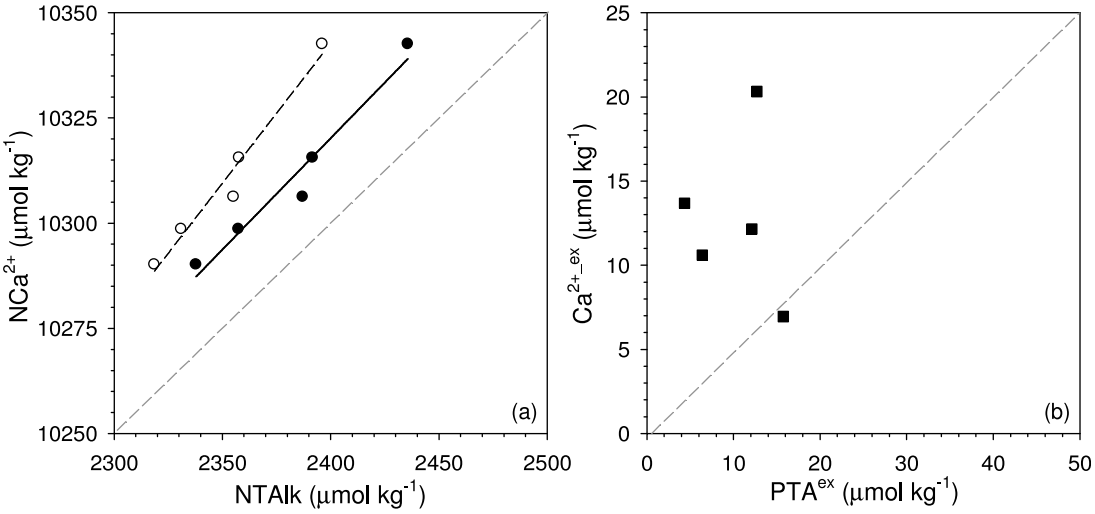

Figure 9. (a) Ca^{2+} versus TAlk (open circles) or PTA (solid circles) in the subsurface water between 200 and 800 m at station SEATS, showing $Ca^{2+} = (0.67 \pm 0.07)TAlk + (8746 \pm 172)$, $r = 0.98$, $n = 5$, and $Ca^{2+} = (0.53 \pm 0.07)PTA + (9050 \pm 157)$, $r = 0.98$, $n = 5$. Note that these data were normalized to a salinity of 35. (b) Excess Ca^{2+} ($Ca^{2+}{}_{-ex}$) versus excess PTA (PTA^{ex}) in the subsurface water between 200 and 800 m at station SEATS. The slope of both gray dashed lines is equal to the theoretical value of 0.5.

apparent Ca^{2+}-TAlk relationship (Figure 9a). On the other hand, underestimation of $CaCO_3$ dissolution might occur if solely using the TAlk data and our study emphasizes the necessity of distinguishing processes influencing Ca^{2+} and TAlk variations. In any case, due to its relatively simpler biogeochemical behavior, comprehensive Ca^{2+} data can give the actual $CaCO_3$ dissolution flux in the ocean potentially advantageous over TAlk, especially since high-precision Ca^{2+} measurements have become routine with advanced instruments such as new generation of automatic potentiometer now commercially available.

5. Conclusions

[38] In the SCS, physical mixing dominated Ca^{2+} distribution, whereas $CaCO_3$ dissolution contributed to the observable gradient. A Ca^{2+} excess of 13 ± 5 μmol kg^{-1} was revealed in the SCS subsurface water relative to the WPS, representing an in situ shallow-depth dissolution rate of ~0.5 mmol m^{-2} d^{-1}. This shallow-depth $CaCO_3$ dissolution might account for as much as half of the total water column dissolution and facilitate the uptake of anthropogenic CO_2 in the upper ocean of the SCS. Moreover, through net subsurface water outflow, this shallow-depth $CaCO_3$ dissolution in the SCS provides significant Ca^{2+} and TAlk export to the open Pacific, which would further improve the capacity to absorb CO_2 in waters along the Kuroshio travel path. In the deep SCS below 1000 m, the amount of Ca^{2+} added from $CaCO_3$ flux relative to its source water (the Southern Ocean) was estimated to be 51 ± 8 μmol kg^{-1}, and this inorganic $CaCO_3$ dissolution contributes ~22% of the DIC increase in the deep water, relative to the decomposition of organic carbon. We envisaged that the significant shallow-depth $CaCO_3$ dissolution in the SCS oversaturated water might be mediated by the microbial oxidation of organic carbon. Further work is needed to understand the coupling and interactions between the oceanic inorganic and organic carbon metabolism.

[39] **Acknowledgments.** This work was supported by the National Basic Research Program of China (973 Program) through grants 2009CB421201 and 2009CB421206 and by the National Science Foundation of China (NSFC) through grants 40821063 and 90711005. We would like to thank Nan Zheng, Xianghui Guo, Lifang Wang, Yan Yang, and Feifei Meng for help with the ancillary data collection and the crew of R/V *Dongfanghong II* and *Shiyan III* for their assistance in sample collection. The 2008 cruise was supported by the South China Sea Institute of Oceanology, the Chinese Academy of Sciences. We thank Dongxiao Wang, Huabin Mao, and Jianyu Hu for providing the CTD data. We are also grateful to the inspiring comments from Shuh-Ji Kao, Wei-Jun Cai, and Chen-Tung Arthur Chen. John Hodgkiss and Harish Gupta are thanked for their help with English. Comments from two anonymous reviewers have significantly improved the quality of the paper.

References

Andersson, A. J., F. T. Mackenzie, and A. Lerman (2005), Coastal ocean and carbonate systems in the high CO_2 world of the Anthropocene, *Am. J. Sci.*, *305*(9), 875–918, doi:10.2475/ajs.305.9.875.

Andersson, A. J., N. R. Bates, and F. T. Mackenzie (2007), Dissolution of carbonate sediments under rising pCO_2 and ocean acidification: Observations from Devil's Hole, Bermuda, *Aquat. Geochem.*, *13*, 237–264, doi:10.1007/s10498-007-9018-8.

Armstrong, R. A., C. Lee, J. I. Hedges, S. Honjo, and S. G. Wakeham (2002), A new, mechanistic model for organic carbon fluxes in the ocean based on the quantitative association of POC with ballast minerals, *Deep Sea Res., Part II*, *49*, 219–236, doi:10.1016/S0967-0645(01)00101-1.

Barker, S., J. A. Higgins, and H. Elderfield (2003), The future of the carbon cycle: Review, calcification response, ballast and feedback on atmospheric CO_2, *Philos. Trans. R. Soc. London, Ser. B*, *361*, 1977–1999.

Beaufort, L., I. Probert, and N. Buchet (2007), Effects of acidification and primary production on coccolith weight: Implications for carbonate transfer from the surface to the deep ocean, *Geochem. Geophys. Geosyst.*, *8*, Q08011, doi:10.1029/2006GC001493.

Berelson, W. M., W. M. Balch, R. Najjar, R. A. Feely, C. Sabine, and K. Lee (2007), Relating estimates of $CaCO_3$ production, export, and dissolution in the water column to measurements of $CaCO_3$ rain into sediment traps and dissolution on the sea floor: A revised global carbonate budget, *Global Biogeochem. Cycles*, *21*, GB1024, doi:10.1029/2006GB002803.

Brewer, P. G., and J. C. Goldman (1976), Alkalinity changes generated by phytoplankton growth, *Limnol. Oceanogr.*, *21*, 108–117, doi:10.4319/lo.1976.21.1.0108.

Brewer, P. G., G. T. F. Wong, M. P. Bacon, and D. W. Spencer (1975), An oceanic calcium problem?, *Earth Planet. Sci. Lett.*, *26*, 81–87, doi:10.1016/0012-821X(75)90179-X.

Cai, L. S. (2007), Geochemistry of settling materials in the northern South China Sea, M. S. thesis, 93 pp., National Sun Yat-Sen Univ., Taiwan.

Cai, W.-J., M. Dai, Y. Wang, W. Zhai, T. Huang, S. Chen, F. Zhang, Z. Chen, and Z. Wang (2004), The biogeochemistry of inorganic carbon and nutrients in the Pearl River estuary and the adjacent northern South China Sea, *Cont. Shelf Res.*, *24*, 1301–1319, doi:10.1016/j.csr.2004.04.005.

Chao, S. Y., P. T. Shaw, and S. Y. Wu (1996), Deep water ventilation in the South China Sea, *Deep Sea Res., Part I*, *43*, 445–466, doi:10.1016/0967-0637(96)00025-8.

Chen, C. T. A. (1983), Distributions of dissolved calcium and alkalinity in the Weddell Sea in winter, *U.S. Antarct. J. Rev.*, 136–137.

Chen, C. T. A. (1990), Rates of calcium carbonate dissolution and organic carbon decomposition in the North Pacific Ocean, *J. Oceanogr.*, *46*, 201–210.

Chen, C. T. A. (1996), The Kuroshio intermediate water is the major source of nutrients on the East China Sea continental shelf, *Oceanol. Acta*, *19*, 523–527.

Chen, C. T. A. (2002), Shelf- vs. dissolution-generated alkalinity above the chemical lysocline, *Deep Sea Res., Part II*, *49*, 5365–5375, doi:10.1016/S0967-0645(02)00196-0.

Chen, C. T. A., and M.-H. Huang (1996), A mid-depth front separating the South China Sea water and the Philippine Sea water, *J. Oceanogr.*, *52*, 17–25, doi:10.1007/BF02236530.

Chen, C. T. A., and R. M. Pytkowicz (1979), On the total CO_2-titration alkalinity-oxygen system in the Pacific Ocean, *Nature*, *281*, 362–365, doi:10.1038/281362a0.

Chen, C. T. A., R. M. Pytkowicz, and E. J. Olson (1982), Evaluation of the calcium problem in the South Pacific, *Geochem. J.*, *16*, 1–10.

Chen, C. T. A., S. L. Wang, B. J. Wang, and S. C. Pai (2001), Nutrient budgets for the South China Sea basin, *Mar. Chem.*, *75*, 281–300, doi:10.1016/S0304-4203(01)00041-X.

Chen, C. T. A., S. L. Wang, W. C. Chou, and D. D. Sheu (2006), Carbonate chemistry and projected future changes in pH and $CaCO_3$ saturation state of the South China Sea, *Mar. Chem.*, *101*, 277–305, doi:10.1016/j.marchem.2006.01.007.

Chen, Y. L. L., and H.-Y. Chen (2006), Seasonal dynamics of primary and new production in the northern South China Sea: The significance of river discharge and nutrient advection, *Deep Sea Res., Part I*, *53*, 971–986, doi:10.1016/j.dsr.2006.02.005.

Chou, W.-C., D. D. Sheu, C. T. A. Chen, L.-S. Wen, Y. Yang, and C.-L. Wei (2007), Transport of the South China Sea subsurface water outflow and its influence on carbon chemistry of Kuroshio waters off southeastern Taiwan, *J. Geophys. Res.*, *112*, C12008, doi:10.1029/2007JC004087.

Culkin, F., and R. A. Cox (1966), Sodium, potassium, magnesium, calcium and strontium in seawater, *Deep Sea Res.*, *13*, 789–804.

Dai, M., F. Meng, T. Tang, S.-J. Kao, J. Lin, J. Chen, J.-C. Huang, J. Tian, J. Gan, and S. Yang (2009), Excess total organic carbon in the intermediate water of the South China Sea and its export to the North Pacific, *Geochem. Geophys. Geosyst.*, *10*, Q12002, doi:10.1029/2009GC002752.

Delille, B., et al. (2005), Response of primary production and calcification to changes of pCO_2 during experimental blooms of the coccolithophorid Emiliania huxleyi, *Global Biogeochem. Cycles*, *19*, GB2023, doi:10.1029/2004GB002318.

de Villiers, S. (1998), Excess dissolved Ca in the deep ocean: A hydrothermal hypothesis, *Earth Planet. Sci. Lett.*, *164*, 627–641, doi:10.1016/S0012-821X(98)00232-5.

de Villiers, S., and B. K. Nelson (1999), Detection of low-temperature hydrothermal fluxes by seawater Mg and Ca anomalies, *Science*, *285*, 721–723, doi:10.1126/science.285.5428.721.

Dittmar, W. (1884), Report on researches into the composition of ocean water collected by H.M.S. *Challenger* during the years 1873–1876, in *Voyage of H.M.S. Challenger*, vol. 1, edited by J. Murray, pp. 1–38, H.M. Stat. Off., London.

Feely, R. A., et al. (2002), In situ calcium carbonate dissolution in the Pacific Ocean, *Global Biogeochem. Cycles*, *16*(4), 1144, doi:10.1029/2002GB001866.

Fennel, K., J. Wilkin, M. Previdi, and R. Najjar (2008), Denitrification effects on air-sea CO_2 flux in the coastal ocean: Simulations for the northwest North Atlantic, *Geophys. Res. Lett.*, *35*, L24608, doi:10.1029/2008GL036147.

Friis, K., R. G. Najjar, M. J. Follows, and S. Dutkiewicz (2006), Possible overestimation of shallow-depth calcium carbonate dissolution in the ocean, *Global Biogeochem. Cycles*, *20*, GB4019, doi:10.1029/2006GB002727.

Friis, K., R. G. Najjar, M. J. Follows, S. Dutkiewicz, A. Körtzinger, and K. M. Johnson (2007), Dissolution of calcium carbonate: Observations and model results in the subpolar North Atlantic, *Biogeosciences*, *4*, 205–213, doi:10.5194/bg-4-205-2007.

Hammond, D. E., P. Giordani, W. M. Berelson, and R. Poletti (1999), Diagenesis of carbon and nutrients and benthic exchange in sediments of the northern Adriatic Sea, *Mar. Chem.*, *66*, 53–79, doi:10.1016/S0304-4203(99)00024-9.

Hernández-Ayon, J. M., A. Zirino, A. G. Dickson, T. Camiro-Vargas, and E. Valenzuela-Espinoza (2007), Estimating the contribution of organic bases from microalgae to the titration alkalinity in costal seawaters, *Limnol. Oceanogr. Methods*, *5*, 225–232.

Honjo, S., J. Dymond, R. Collier, and S. J. Manganini (1995), Export production of particles to the interior of equatorial Pacific Ocean during 1992 EqPac experiment, *Deep Sea Res., Part II*, *42*, 831–870, doi:10.1016/0967-0645(95)00034-N.

Huang, K.-F., C.-F. You, H.-L. Lin, and Y.-T. Shieh (2008), In situ calibration of Mg/Ca ratio in planktonic foraminiferal shell using time series sediment trap: A case study of intense dissolution artifact in the South China Sea, *Geochem. Geophys. Geosyst.*, *9*, Q04016, doi:10.1029/2007GC001660.

Ikegami, H., and S. Kanamori (1983), Calcium-alkalinity-nitrate relationship in the North Pacific and the Japan Sea, *J. Oceanogr.*, *39*, 9–14.

Intergovernmental Panel on Climate Change (2007), Summary for policymakers, in *Climate Change 2007: The Physical Science Basis. Contribution of Working Group I to the Fourth Assessment Report of the Intergovernmental Panel on Climate Change*, edited by S. Solomon et al., pp. 1–18, Cambridge Univ. Press, Cambridge, U. K.

Johnson, D. R., T. P. Boyer, H. E. Garcia, R. A. Locarnini, A. V. Mishonov, M. T. Pitcher, O. K. Baranova, J. I. Antonov, and I. V. Smolyar (2006), *World Ocean Database 2005 Documentation. NODC Internal Report 18*, edited by S. Levitus, U.S. Govt. Print. Off., Washington, D. C.

Kanamori, S., and H. Ikegami (1980), Computer-processed potentiometric titration for the determination of calcium and magnesium in sea water, *J. Oceanogr.*, *36*, 177–184.

Kanamori, S., and H. Ikegami (1982), Calcium-alkalinity relationship in the North Pacific, *J. Oceanogr.*, *38*, 57–62.

Kim, H.-C., and K. Lee (2009), Significant contribution of dissolved organic matter to seawater alkalinity, *Geophys. Res. Lett.*, *36*, L20603, doi:10.1029/2009GL040271.

Kleypas, J. A., R. W. Buddemeier, D. Archer, J.-P. Gattuso, C. Langdon, and B. N. Opdyke (1999), Geochemical consequences of increased atmospheric carbon dioxide on coral reefs, *Science*, *284*, 118–120, doi:10.1126/science.284.5411.118.

Lebel, J., and A. Poisson (1976), Potentiometric determination of calcium and magnesium in seawater, *Mar. Chem.*, *4*, 321–332, doi:10.1016/0304-4203(76)90018-9.

Li, L., and T. D. Qu (2006), Thermohaline circulation in the deep South China Sea basin inferred from oxygen distributions, *J. Geophys. Res.*, *111*, C05017, doi:10.1029/2005JC003164.

Liu, K.-K., S.-Y. Chao, P.-T. Shaw, G.-C. Gong, C.-C. Chen, and T. Y. Tang (2002), Monsoon-forced chlorophyll distribution and primary production in the South China Sea: Observations and a numerical study, *Deep Sea Res., Part I*, *49*, 1387–1412, doi:10.1016/S0967-0637(02)00035-3.

Liu, C.-T., R. Pinkel, M.-K. Hsu, J. M. Klymak, H.-W. Chen, and C. Villanoy (2006), Nonlinear internal waves from the Luzon Strait, *EOS Trans. AGU*, *87*(42), 449–451, doi:10.1029/2006EO420002.

Martin, J. H., S. E. Fitzwater, R. M. Gordon, C. N. Hunter, and S. J. Tanner (1993), Iron, primary production and carbon-nitrogen flux studies during the JGOFS North Atlantic bloom experiment, *Deep Sea Res., Part II*, *40*, 115–134, doi:10.1016/0967-0645(93)90009-C.

Millero, F. J. (2006), Composition of the major components of seawater, in *Chemical Oceanography*, 3rd ed., chap. 2, pp. 55–88, CRC Press, Boca Raton, Fla.

Millero, F. J. (2007), The marine inorganic carbon cycle, *Chem. Rev.*, *107*, 308–341, doi:10.1021/cr0503557.

Milliman, J. D. (1993), Production and accumulation of calcium carbonate in the ocean: Budget of an unsteady state, *Global Biogeochem. Cycles*, *7*(4), 927–957, doi:10.1029/93GB02524.

Milliman, J. D., and A. W. Droxler (1996), Neritic and pelagic carbonate sedimentation in the marine environment: Ignorance is not bliss, *Geol. Rundsch.*, *85*, 496–504, doi:10.1007/BF02369004.

Milliman, J. D., P. J. Troy, W. M. Balch, A. K. Adams, Y.-H. Li, and F. T. Mackenzie (1999), Biologically mediated dissolution of calcium carbonate above the chemical lysocline?, *Deep Sea Res., Part I*, *46*, 1653–1669, doi:10.1016/S0967-0637(99)00034-5.

Moore, J. K., S. C. Doney, D. M. Glover, and I. Y. Fung (2002), Iron cycling and nutrient-limitation patterns in surface waters of the world ocean, *Deep Sea Res., Part II*, *49*, 463–507, doi:10.1016/S0967-0645(01)00109-6.

Moore, J. K., S. C. Doney, and K. Lindsay (2004), Upper ocean ecosystem dynamics and iron cycling in a global three-dimensional model, *Global Biogeochem. Cycles*, *18*, GB4028, doi:10.1029/2004GB002220.

Morse, J. W. (1974), Dissolution kinetics of calcium carbonate in seawater. V. Effects of natural inhibitors and the position of the chemical lysocline, *Am. J. Sci.*, *274*, 638–647, doi:10.2475/ajs.274.6.638.

Olson, E. J., and C. T. A. Chen (1982), Interference in the determination of calcium in seawater, *Limnol. Oceanogr.*, *27*(2), 375–380, doi:10.4319/lo.1982.27.2.0375.

Orr, J. C., et al. (2005), Anthropogenic ocean acidification over the twenty-first century and its impact on calcifying organisms, *Nature*, *437*, 681–686, doi:10.1038/nature04095.

Pilson, M. E. Q. (1998), Major constituents of seawater, in *An Introduction to the Chemistry of the Sea*, chap. 4, pp. 58–65, Prentice Hall, Upper Saddle River, N. J.

Qu, T. D., J. B. Girton, and J. A. Whitehead (2006), Deepwater overflow through Luzon Strait, *J. Geophys. Res.*, *111*, C01002, doi:10.1029/2005JC003139.

Riebesell, U., I. Zondervan, B. Rost, P. D. Tortell, R. E. Zeebe, and F. M. M. Morel (2000), Reduced calcification of marine plankton in response to increased atmospheric CO_2, *Nature*, *407*, 364–367, doi:10.1038/35030078.

Riley, J. P., and M. Tongudai (1967), The major cation/chlorinity ratios in seawater, *Chem. Geol.*, *2*, 263–269, doi:10.1016/0009-2541(67)90026-5.

Sagi, T. (1969), The concentration of calcium and the calcium chlorosity ratio in the western North Pacific Ocean, *Oceanogr. Mag.*, *21*, 61–66.

Sheu, D. D., W.-C. Chou, C. T. A. Chen, C.-L. Wei, H.-L. Hsieh, W.-P. Hou, and M. Dai (2009), Riding over the Kuroshio from the South to the East China Sea: Mixing and transport of DIC, *Geophys. Res. Lett.*, *36*, L07603, doi:10.1029/2008GL037017.

Shiller, A. M., and J. M. Gieskes (1980), Processes affecting the oceanic distributions of dissolved calcium and alkalinity, *J. Geophys. Res.*, *85*, 2719–2727, doi:10.1029/JC085iC05p02719.

Thomas, H., L.-S. Schiettecatte, K. Suykens, Y. J. M. Koné, E. H. Shadwick, A. E. F. Prowe, Y. Bozec, H. J. W. de Baar, and A. V. Borges (2009), Enhanced ocean carbon storage from anaerobic alkalinity generation in coastal sediments, *Biogeosciences*, *6*, 267–274, doi:10.5194/bg-6-267-2009.

Tian, J. W., Q. X. Yang, X. F. Liang, L. L. Xie, D. X. Hu, F. Wang, and T. D. Qu (2006), Observation of Luzon Strait transport, *Geophys. Res. Lett.*, *33*, L19607, doi:10.1029/2006GL026272.

Tsunogai, S., M. Nishimura, and S. Nakaya (1968), Calcium and magnesium in sea water and the ratio of calcium to chlorinity as a tracer of water masses, *J. Oceanogr.*, *24*, 153–159.

Tsunogai, S., T. Yamazaki, and M. Nishimura (1971), Calcium in the Antarctic Ocean, *J. Oceanogr.*, *27*, 191–196.

Tsunogai, S., H. Yamahata, S. Kudo, and O. Saito (1973), Calcium in the Pacific Ocean, *Deep Sea Res.*, *20*, 717–726.

Wolf-Gladrow, D. A., R. E. Zeebe, C. Klaas, A. Körtzinger, and A. G. Dickson (2007), Total alkalinity: The explicit conservative expression and its application to biogeochemical processes, *Mar. Chem.*, *106*, 287–300, doi:10.1016/j.marchem.2007.01.006.

Wollast, R., and L. Chou (1998), Distribution and fluxes of calcium carbonate along the continental margin in the Gulf of Biscay, *Aquat. Geochem.*, *4*, 369–393, doi:10.1023/A:1009640432692.

Wollast, R., and L. Chou (2001), The carbon cycle at the ocean margin in the northern Gulf of Biscay, *Deep Sea Res., Part II*, *48*, 3265–3293, doi:10.1016/S0967-0645(01)00040-6.

Wong, C. S., F. A. Whitney, D. W. Crawford, K. Iseki, R. J. Matear, W. K. Johnson, J. S. Page, and D. Timothy (1999), Seasonal and interannual variability in particle fluxes of carbon, nitrogen and silicon from times series of sediment traps at Ocean Station P, 1982–1983: Relationship to changes in subarctic primary productivity, *Deep Sea Res., Part II*, *46*, 2735–2760, doi:10.1016/S0967-0645(99)00082-X.

Wong, G. T. F., T.-L. Ku, M. Mulholland, C.-M. Tseng, and D.-P. Wang (2007), The South East Asian Time-series Study (SEATS) and the biogeochemistry of the South China Sea: An overview, *Deep Sea Res., Part II*, *54*, 1434–1447, doi:10.1016/j.dsr2.2007.05.012.

Zondervan, I., R. E. Zeebe, B. Rost, and U. Riebesell (2001), Decreasing marine biogenic calcification: A negative feedback on rising atmospheric pCO_2, *Global Biogeochem. Cycles*, *15*(2), 507–516, doi:10.1029/2000GB001321.

Z. Cao and M. Dai, State Key Laboratory of Marine Environmental Science, Xiamen University, 422 Simingnanlu, Xiamen 361005, China. (mdai@xmu.edu.cn)